



Schweizerischer Erdbebendienst  
Service Sismologique Suisse  
Servizio Sismico Svizzero  
Servizi da Terratrembels Svizzer



Eidgenössische Technische Hochschule Zürich  
Swiss Federal Institute of Technology Zurich

---

# **Locarno - Pompieri (SLOP)**

## **SITE CHARACTERIZATION REPORT**

**Clotaire MICHEL, Daniel ROTEN, Carlo CAUZZI**

**Valerio POGGI, Jan BURJANEK, Donat FÄH**

---



Sonneggstrasse 5 CH-8092 Zürich Switzerland; E-mail: [clotaire.michel@sed.ethz.ch](mailto:clotaire.michel@sed.ethz.ch)

Last modified : November 5, 2013

## Abstract

Ambient vibration array measurements were performed to characterize the site Locarno Pompiéri. The site, where the new station SLOP of the Swiss Strong Motion Network was installed, is located on the alluvial fan of the Maggia river in the lake Maggiore basin. An H/V survey in the city of Locarno was first performed to understand the variability of the seismic response. It was found that the sediment thickness in the city of Locarno is driving the fundamental H/V peak frequency, down to 0.3 Hz, corresponding probably to more than 800 m of sediments. At the SLOP site, the H/V peak is at 0.67 Hz. In order to characterize the velocity profile under the station, array measurements with a 320 m aperture were performed. The measurements were successful and allowed deriving a velocity model for this site. The soil column underlying station SLOP does not show clear interfaces. The first 10 – 20 m are made of unconsolidated sand with few gravels with a velocity slightly below 300 m/s. The velocity remains around 500 m/s down to 100 m depth. It reaches 800 m/s at 200 m depth and 1000 m/s at 400 m depth. The interface with the bedrock is not well constrained and between 400 and 550 m depth.  $V_{s,30}$  is 304 m/s, which would corresponds to ground type C in the Eurocode 8 [CEN, 2004] and SIA261 [SIA, 2003]. The theoretical 1D SH transfer function and impedance contrast of the quarter-wavelength velocity computed from the inverted profiles show amplifications at clear resonance frequencies, especially at 1.1, 1.8 and 2.5 Hz. Recordings on the new station will allow to compare to these simple models.

<i>CONTENTS</i>	3
<b>Contents</b>	
<b>1 Introduction</b>	<b>4</b>
<b>2 Experiment description</b>	<b>5</b>
2.1 Ambient Vibrations . . . . .	5
2.2 Equipment . . . . .	5
2.3 Location of the recordings . . . . .	5
2.4 Positioning of the stations . . . . .	6
<b>3 Data quality</b>	<b>8</b>
3.1 Usable data . . . . .	8
3.2 Data processing . . . . .	8
<b>4 H/V processing</b>	<b>10</b>
4.1 Processing method and parameters . . . . .	10
4.2 Results in the city of Locarno . . . . .	10
4.3 Results in the array . . . . .	10
4.4 Polarization analysis . . . . .	11
<b>5 Array processing</b>	<b>14</b>
5.1 Processing methods and parameters . . . . .	14
5.2 Obtained dispersion curves . . . . .	14
<b>6 Inversion and interpretation</b>	<b>16</b>
6.1 Inversion . . . . .	16
6.2 Travel time average velocities and ground type . . . . .	20
6.3 SH transfer function and quarter-wavelength velocity . . . . .	21
<b>7 Conclusions</b>	<b>24</b>
<b>References</b>	<b>26</b>

# 1 Introduction

The station SLOP (Locarno - Pompieri) is part of the Swiss Strong Motion Network (SSMNet). It is located in a developing zone of the city hosting several departments of the administration, the fire brigades and several schools. SLOP has been installed in the framework of the SSM-Net Renewal project in 2013 as a new site. This project includes also the site characterization. Passive array measurements have been selected as a standard tool to investigate these sites. An array measurement campaign was carried out on 24st May 2013 around the Via alla Peschiera (Fig. 1), with a centre close to station SLOP, in order to characterize the velocity profile under this station. This station is located on the Maggia alluvial fan, in the basin of the lake Maggiore. A single-station measurement campaign was also performed on the alluvial fan to understand the variability of the resonance frequencies in the city. This report presents the measurement setup, the results of the H/V analysis and of the array processing of the surface waves (dispersion curves). Then, an inversion of these results into velocity profiles is performed. Standard parameters are derived to evaluate the amplification at this site.

Canton	City	Location	Station code	Site type	Slope
Ticino	Locarno	Pompieri	SLOP	Deep valley	Flat

Table 1: Main characteristics of the study-site.



Figure 1: Picture of the site.

## 2 Experiment description

### 2.1 Ambient Vibrations

The ground surface is permanently subjected to ambient vibrations due to:

- natural sources (ocean and large-scale atmospheric phenomena) below 1 Hz,
- local meteorological conditions (wind and rain) at frequencies around 1 Hz ,
- human activities (industrial machines, traffic...) at frequencies above 1 Hz [Bonney-Claudet et al., 2006].

The objective of the measurements is to record these ambient vibrations and to use their propagation properties to infer the underground structure. First, the polarization of the recorded waves (H/V ratio) is used to derive the resonance frequencies of the soil column. Second, the arrival time delays at many different stations are used to derive the velocity of surface waves at different frequencies (dispersion). The information (H/V, dispersion curves) is then used to derive the properties of the soil column using an inversion process.

### 2.2 Equipment

For single-station measurements, 1 Quanterra Q330 data logger and 1 Lennartz 3C 5s seismometer were used. The time was not corrected by GPS and can be different from the GPS time by several minutes. The sensor was generally directly placed on asphalt.

For the array measurements 11 Quanterra Q330 dataloggers named NR01 to NR12 (except NR08) and 14 Lennartz 3C 5 s seismometers were available (see Tab. 2). Each datalogger can record on 2 ports A (channels EH1, EH2, EH3 for Z, N, E directions) and B (channels EH4, EH5, EH6 for Z, N, E directions). Time synchronization was ensured by GPS. The sensors were placed on a metal tripod, in a 20 cm deep hole, when possible, for better coupling with the ground.

Survey	Digitizer	Model	Number	Resolution
Array		Quanterra Q330	11	24 bits
Single station		Quanterra Q330	1	24 bits
Survey	Sensor type	Model	Number	Cut-off frequency
Array	Velocimeter	Lennartz 3C	14	0.2 Hz
Single station	Velocimeter	Lennartz 3C	1	0.2 Hz

Table 2: Equipment used.

### 2.3 Location of the recordings

Two array configurations were used, for a total of 4 rings of 10, 30, 80 and 160 m radius around a central station. The first configuration includes the 3 inner rings with 14 sensors; the second

configuration includes the 2 outer rings (plus 1 sensor of the first ring) with 12 sensors. The minimum inter-station distance and the aperture are therefore 10 and 160 m and 10 and 320 m, respectively. The experimental setup is displayed in Fig. 2. The final usable datasets are detailed in section 3.2.

The single station campaign aimed at measuring on a grid covering the city centre (Fig. 3).

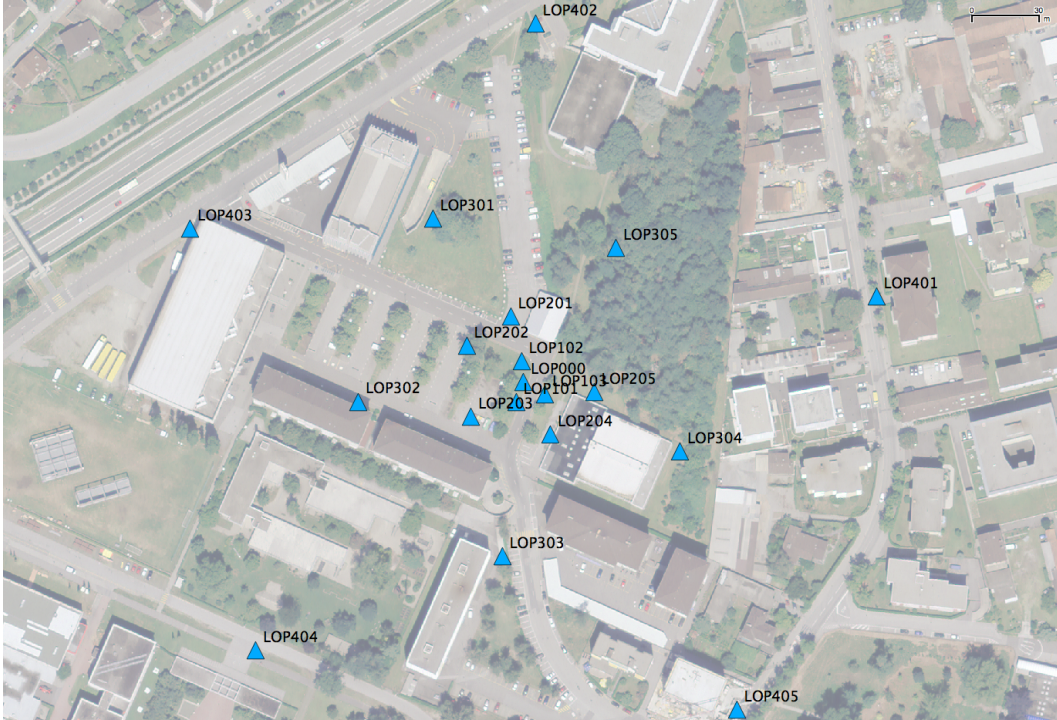


Figure 2: Geometry of the arrays.

## 2.4 Positioning of the stations

For the array measurement, the sensor coordinates were measured using a differential GPS device (Leica Viva GS10), including only a rover station and using the Real Time Kinematic technique provided by Swisstopo. It allows an absolute positioning with an accuracy better than 7 cm on the Swissgrid. However, this accuracy was not reached at some points (LOP305 with 26 cm and LOP401 with 19 cm).

For the single station campaign, the positioning was done by picking location on the 1:25000 map, with an accuracy of 5 m.

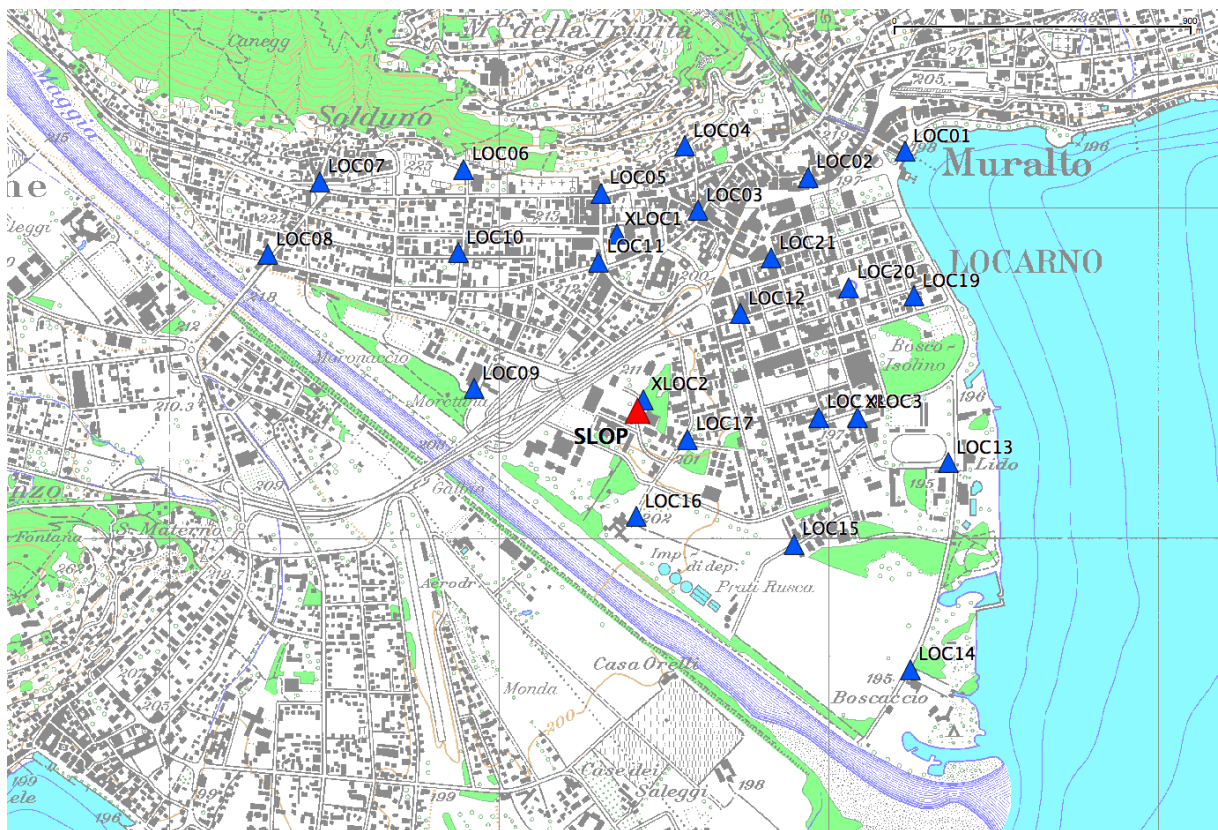


Figure 3: Position of the single station measurements.

## 3 Data quality

### 3.1 Usable data

The largest time windows were extracted, for which all the sensors of the array were correctly placed and the GPS synchronization was ensured. The array was limited in size by the highway in the North. The quality of the datasets is good without particular disturbances, except a light traffic and some pedestrians. The battery at point LOP303 failed in the middle of dataset 2 so that only 11 points are available for this dataset.

Orientations of the sensors were checked by maximizing the correlation with the central station at low frequencies [Poggi et al., 2012b]. Surprisingly large deviations were found, especially for points LOP302 (30°), LOP401 (26°), LOP103 (18°), LOP402 (14°), LOP404 (13°), LOP303, LOP305, LOP301 ( $\approx 10^\circ$ ). Original and rotated datasets are available for the 3C array analysis.

For the single station campaign, ambient vibrations were recorded during approximately 30 min at each point.

The characteristics of the datasets are detailed in Tab. 3.

### 3.2 Data processing

The data were first converted to SAC format including in the header the coordinates of the point (CH1903 system), the recording component and a name related to the position. The name for the array points is made of 3 letters characterizing the location (LOP here), 1 digit for the ring and 2 more digits for the number in the ring. For the single station measurement, the three letters are LOC and the numbers are increasing from 001 to 021. It should be noticed that additional temporary stations XLOC1, 2 and 3 were processed as well in this report. Recordings were not corrected for instrumental response.

<b>Dataset</b>	<b>Starting Date</b>	<b>Time</b>	<b>Length</b>	$F_s$	<b>Min. inter-distance</b>	<b>Aperture</b>	<b># of points</b>
1	2013/05/24	11:04	90 min	200 Hz	10 m	160 m	14
2	2013/05/24	13:10	124 min	200 Hz	10 m	320 m	11
LOC01	2012/06/14	07:34	34 min	200 Hz			1
LOC02	2012/06/14	08:29	31 min	200 Hz			1
LOC03	2012/06/14	09:21	29 min	200 Hz			1
LOC04	2012/06/14	10:10	28 min	200 Hz			1
LOC05	2012/06/14	10:57	30 min	200 Hz			1
LOC06	2012/06/14	11:50	28 min	200 Hz			1
LOC07	2012/06/14	12:40	30 min	200 Hz			1
LOC08	2012/06/14	13:24	29 min	200 Hz			1
LOC09	2012/06/14	14:19	29 min	200 Hz			1
LOC10	2012/06/14	15:08	30 min	200 Hz			1
LOC11	2012/06/14	15:59	29 min	200 Hz			1
LOC12	2012/06/14	16:49	28 min	200 Hz			1
LOC13	2012/06/15	05:48	33 min	200 Hz			1
LOC14	2012/06/15	06:38	29 min	200 Hz			1
LOC15	2012/06/15	07:28	30 min	200 Hz			1
LOC16	2012/06/15	08:21	29 min	200 Hz			1
LOC17	2012/06/15	09:04	29 min	200 Hz			1
LOC18	2012/06/15	09:58	29 min	200 Hz			1
LOC19	2012/06/15	10:44	28 min	200 Hz			1
LOC20	2012/06/15	11:27	28 min	200 Hz			1
LOC21	2012/06/15	12:11	30 min	200 Hz			1

Table 3: Usable datasets.

## 4 H/V processing

### 4.1 Processing method and parameters

In order to process the H/V spectral ratios, several codes and methods were used. The classical H/V method was applied using the Geopsy <http://www.geopsy.org> software. In this method, the ratio of the smoothed Fourier Transform of selected time windows are averaged. Tukey windows (cosine taper of 5% width) of 50 s long overlapping by 50% were selected. Konno and Ohmachi [1998] smoothing procedure was used with a b value of 60. The classical method computed using the method of Fäh et al. [2001] was also performed.

Moreover, the time-frequency analysis method [Fäh et al., 2009] was used to estimate the ellipticity function more accurately using the Matlab code of V. Poggi. In this method, the time-frequency analysis using the Wavelet transform is computed for each component. For each frequency, the maxima over time (10 per minute with at least 0.1 s between each) in the TFA are determined. The Horizontal to Vertical ratio of amplitudes for each maximum is then computed and statistical properties for each frequency are derived. A Cosine wavelet with parameter 9 is used. The mean of the distribution for each frequency is stored. For the sake of comparison, the time-frequency analysis of Fäh et al. [2001], based on the spectrogram, was also used, as well as the wavelet-based TFA coded in Geopsy.

The ellipticity extraction using the Capon analysis [Poggi and Fäh, 2010] (see section on array analysis) was also performed.

Method	Freq. band	Win. length	Anti-trig.	Overlap	Smoothing
Standard H/V Geopsy	0.2 – 20 Hz	50 s	No	50%	K&O 60
Standard H/V D. Fäh	0.2 – 20 Hz	30 s	No	75%	-
H/V TFA Geopsy	0.2 – 20 Hz	Morlet m=8 fi=1	No	-	-
H/V TFA D. Fäh	0.2 – 20 Hz	Specgram	No	-	-
H/V TFA V. Poggi	0.2 – 20 Hz	Cosine wpar=9	No	-	No

Table 4: Methods and parameters used for the H/V processing.

### 4.2 Results in the city of Locarno

The fundamental frequency in the H/V analysis is presented on Fig. 4. It shows a clear gradient from the shallow sediments close to the rock outcrop in the North to the lake shore, where it drops down to 0.3 Hz. This gradient is mostly explained by the rock dipping at  $40^\circ$  below the sediments of the Maggia delta and the lake Maggiore. The old town shows values around 1 – 1.5 Hz, whereas the region of the station SLOP is about 0.6 – 0.7 Hz.

### 4.3 Results in the array

All points of the 3 inner rings show the same shape in their H/V with a clear fundamental peak at 0.67 Hz. In the outer ring, the fundamental frequency starts to change slightly with the largest

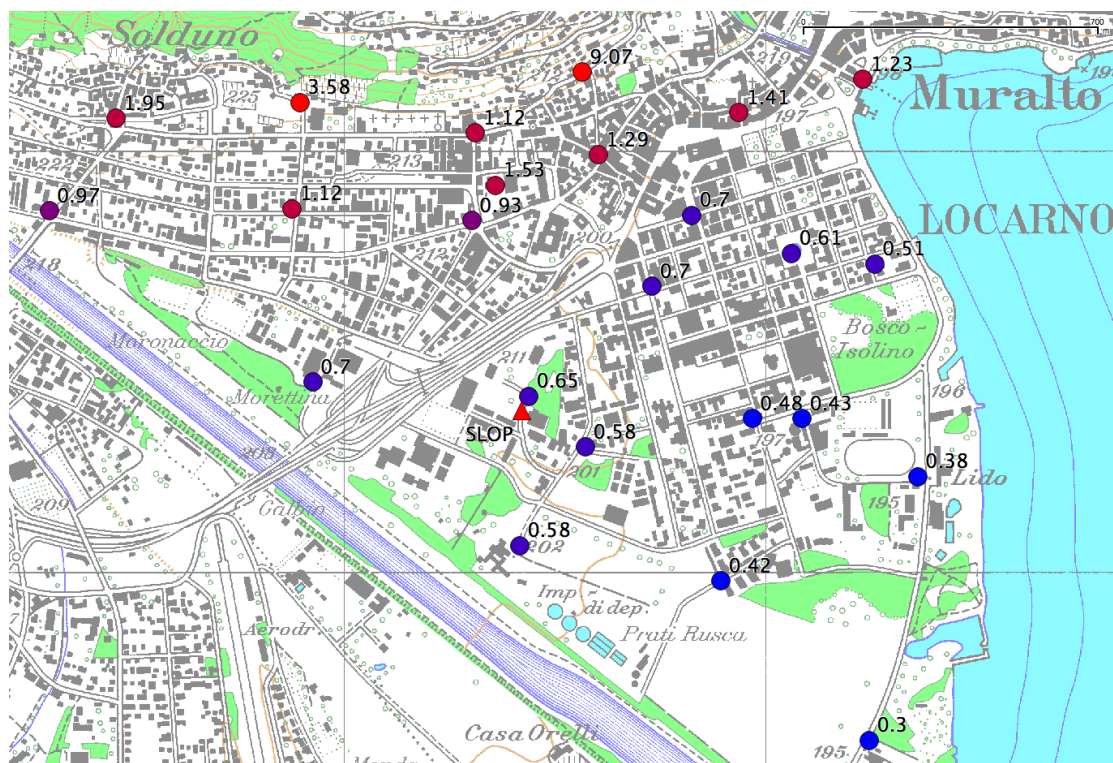


Figure 4: Map of the fundamental H/V peak in the city of Locarno with frequencies in Hz.

values in the North (Fig. 7).

Moreover, all the methods to compute H/V ratios are compared at the array centre on Fig. 6, in which the classical methods were divided by  $\sqrt{2}$  to correct from the Love wave contribution [Fäh et al., 2001]. The classical and TFA methods match well, except for the amplitude of the fundamental frequency. The 3C FK analysis (Capon method) does not have resolution down to the peak but the right flank matches well.

The fundamental peak at the SLOP station is therefore at 0.67 Hz, with a peak amplitude around 5 for the TFA methods.

#### 4.4 Polarization analysis

Considering the shape of the Lake Maggiore basin, a 2D resonance could occur. Therefore, polarization analysis on the array data was performed using the method of Burjánek et al. [2010]. Most of the points (Fig. 8) show a weak polarization at 0.6 Hz in the ENE-WNW direction, i.e. the direction of the slope of the alluvial fan. Therefore, 2D effects are not excluded at this site, but not related to the Lake Maggiore basin.

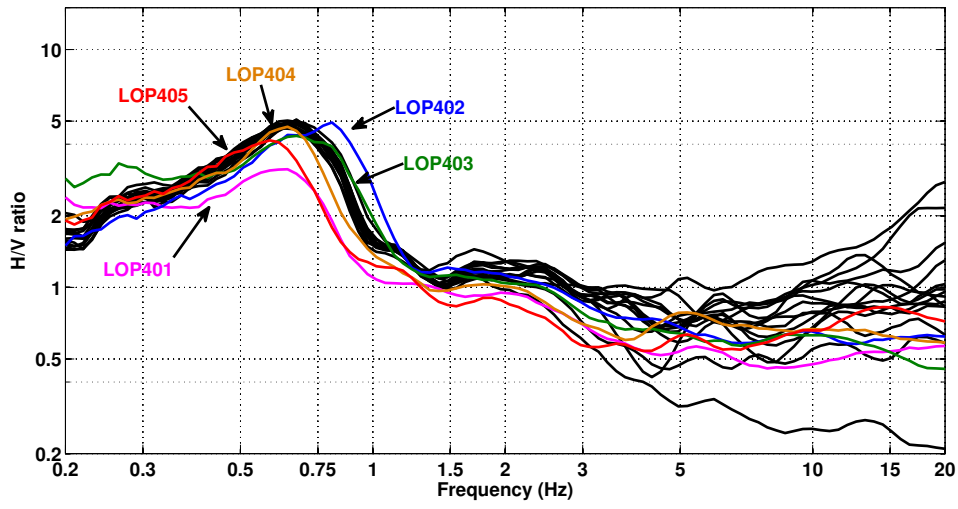


Figure 5: H/V spectral ratios (time-frequency analysis code V. Poggi).

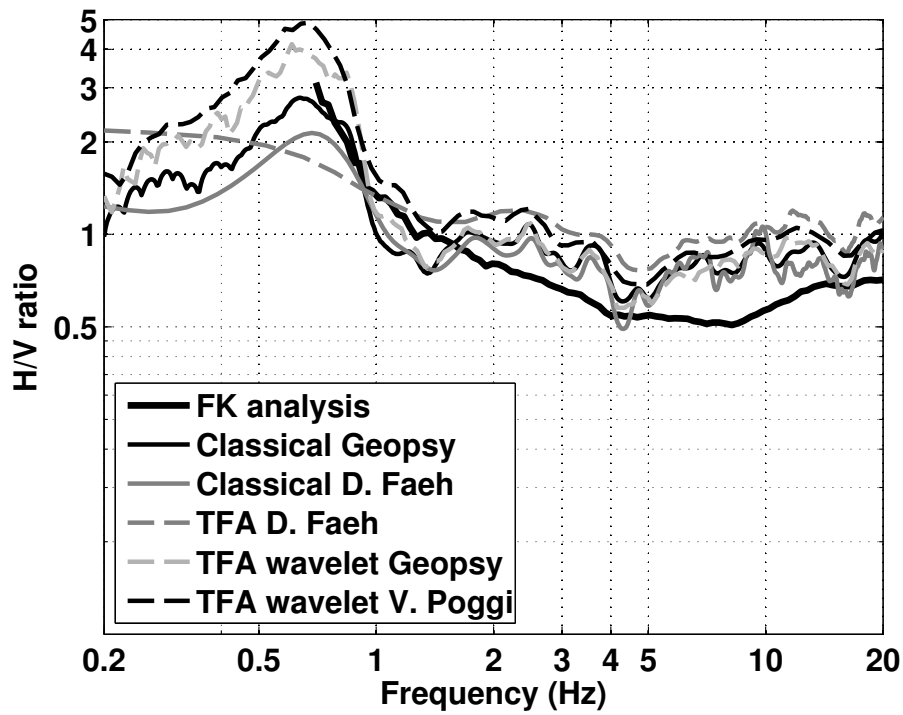


Figure 6: H/V spectral ratios for point LOP000 using the different codes. Classical methods were divided by  $\sqrt{2}$ .

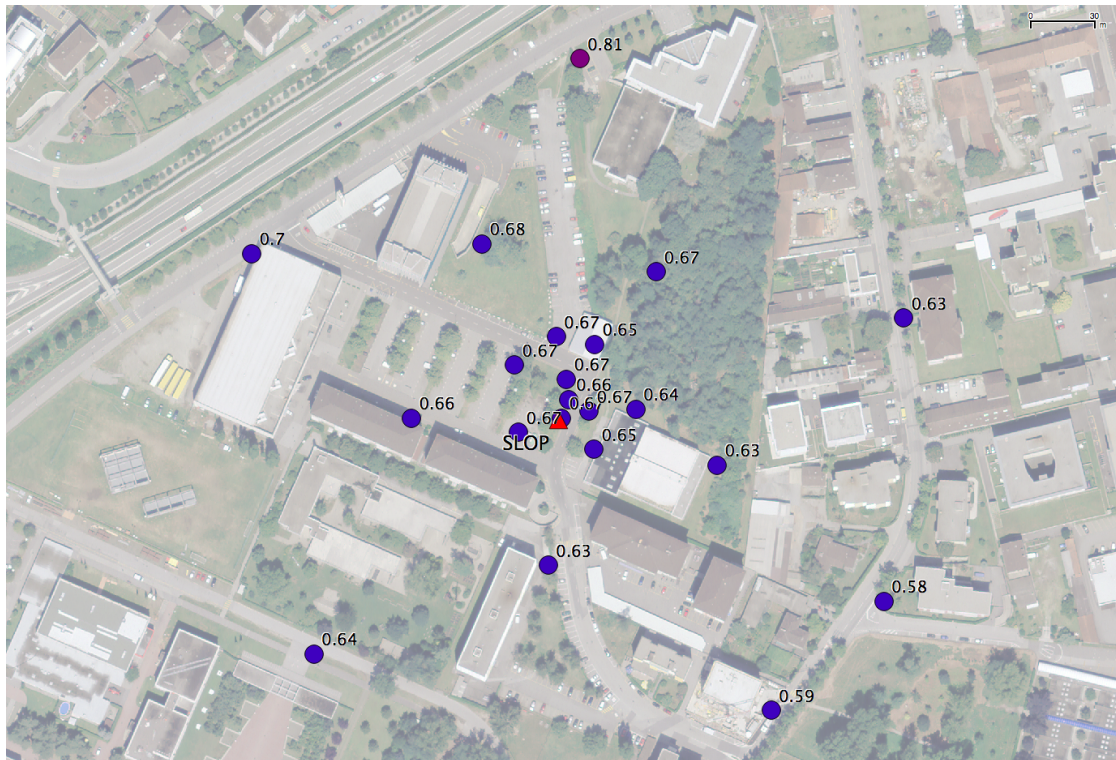


Figure 7: Map of the fundamental peak in the H/V in the array with frequencies in Hz.

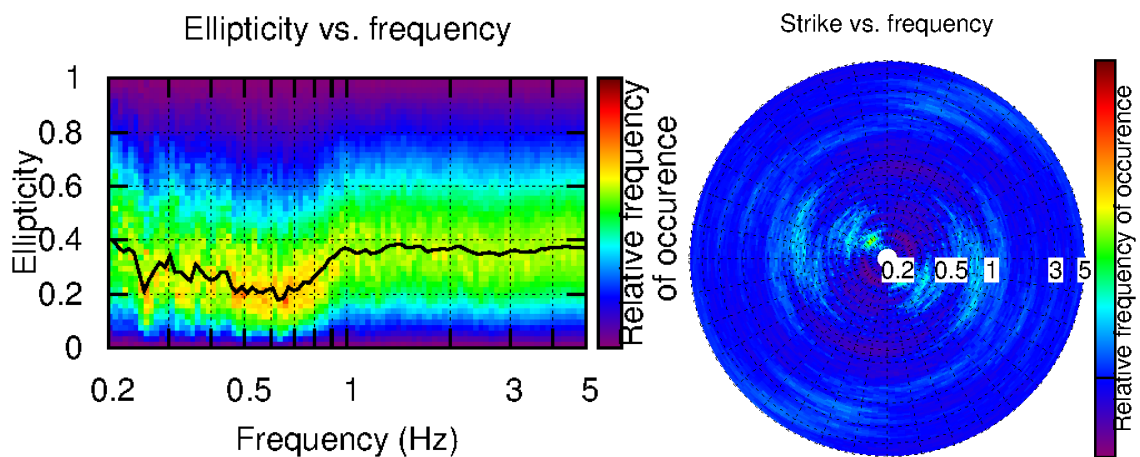


Figure 8: Polarization analysis at point LOP000. Left: Ellipticity (A trough in the ellipticity corresponds to polarized motion). Right: Strike of the polarization.

## 5 Array processing

### 5.1 Processing methods and parameters

The vertical components of the arrays were processed using the FK and the High-resolution FK analysis [Capon, 1969] using the Geopsy <http://www.geopsy.org> software. Better results were obtained using large time windows (300T). The results of computations of both datasets were merged to estimate the dispersion curves.

Moreover, a 3C array analysis [Fäh et al., 2008] was also performed using the `array_tool_3C` software [Poggi and Fäh, 2010]. It allows to derive Rayleigh and Love modes including the Rayleigh ellipticity. The results of computations of both datasets were merged to estimate the dispersion curves.

Method	Set	Freq. band	Win. length	Anti-trig.	Overlap	Grid step	Grid size	# max.
HRFK 1C	1	0.5 – 20 Hz	300T	No	50%	0.001	0.6	5
HRFK 1C	2	0.5 – 20 Hz	300T	No	50%	0.001	0.6	5
HRFK 3C	1	0.5 – 20 Hz	Wav. 10 Tap. 0.2	No	50%	150 m/s	2500 m/s	5
HRFK 3C	2	0.5 – 20 Hz	Wav. 10 Tap. 0.2	No	50%	150 m/s	2500 m/s	5

Table 5: Methods and parameters used for the array processing.

### 5.2 Obtained dispersion curves

The first Rayleigh mode in the 1C FK analysis could be picked between 1 and 14 Hz (Fig. 9) including its standard deviation. The velocities are ranging from 1100 m/s at 1 Hz down to 260 m/s at 14 Hz.

Using the 3C analysis, both fundamental Rayleigh and Love modes can be picked (Fig. 9). Rayleigh fundamental mode is picked from 1.2 to 15 Hz and Love from 0.9 to 4.3 Hz with confidence and up to 11.5 Hz with less certainty. A higher Love mode is picked on a short frequency band as well.

All picked curves are presented together on Fig. 10. Rayleigh curves from the two picking match perfectly.

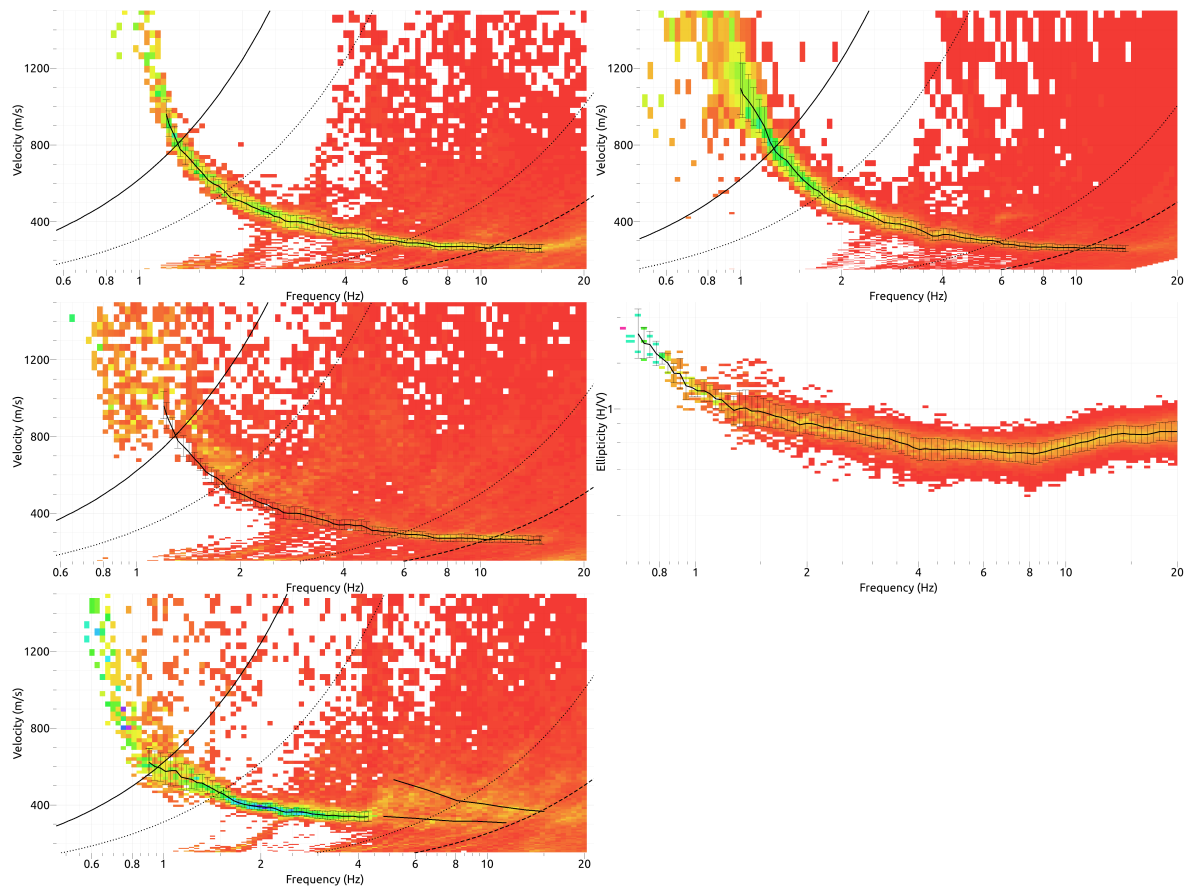


Figure 9: Dispersion curves obtained from the 3C (left) and 1C (top right) array analysis (from top to bottom: vertical, radial, transverse components and ellipticity) and ellipticity from the 3C analysis (centre right).

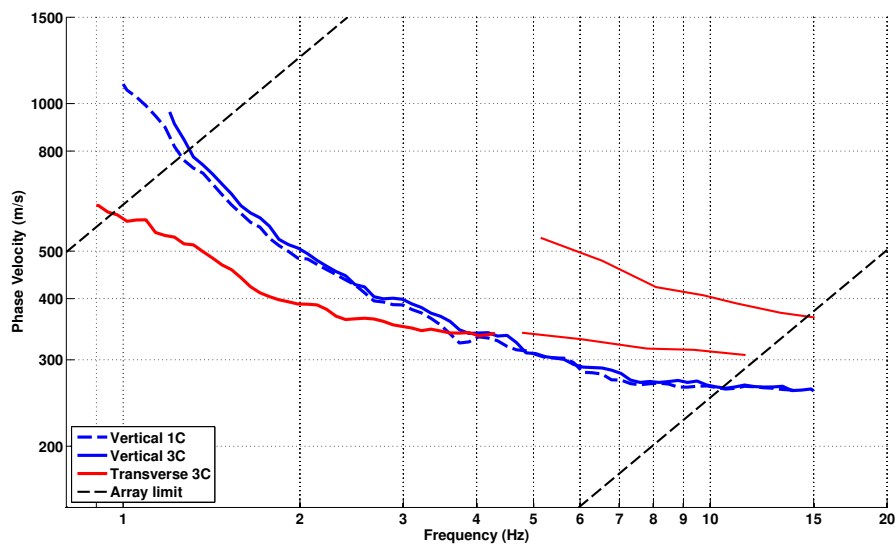


Figure 10: Picked dispersion curves from 1C and 3C FK methods.

## 6 Inversion and interpretation

### 6.1 Inversion

For the inversion, Rayleigh and Love fundamental and Love first higher modes dispersion curves, as well as the right flank of the ellipticity and the fundamental frequency at 0.67 Hz were used as simultaneous targets without standard deviation to avoid different weighting. Love fundamental mode above 4 Hz was not used. A weight of 0.2 was assigned to the ellipticity curve and the ellipticity peak. All curves were resampled using 50 points between 0.5 and 20 Hz in log scale.

The inversion was performed using the Improved Neighborhood Algorithm (NA) Wathelet [2008] implemented in the Dinver software. In this algorithm, the tuning parameters are the following:  $N_{s_0}$  is the number of starting models, randomly distributed in the parameter space,  $N_r$  is the the number of best cells considered around these  $N_{s_0}$  models,  $N_s$  is the number of new cells generated in the neighborhood of the  $N_r$  cells ( $N_s/N_r$  per cell) and  $It_{max}$  is the number of iteration of this process. The process ends with  $N_{s_0} + N_r * \frac{N_s}{N_r} * It_{max}$  models. The used parameters are detailed in Tab. 6.

$It_{max}$	$N_{s_0}$	$N_s$	$N_r$
500	10000	100	100

Table 6: Tuning parameters of Neighborhood Algorithm.

Low velocity zones were not allowed in the inversion, although it cannot be excluded that lake sediments lay below the fluvial sediments. The Poisson ratio was inverted in each layer in the range 0.2-0.4, up to 0.47 in the upper layers, i.e. within the expected groundwater table. The density was assumed to be 2000 kg/m<sup>3</sup> in the upper layers and 2500 kg/m<sup>3</sup>. Inversions with free layer depths as well as fixed layer depths were performed. More layers than needed are used to smooth the obtained results and better explore the parameter space. 5 independent runs of 5 different parametrization schemes (6 and 7 layers over a half space and 10, 11 and 12 layers with fixed depth) were performed. For further elaborations, the best models of these 25 runs were selected (Fig. 14).

The retrieved velocity profiles show a velocity gradient without clear interface. The first 10 – 20 m have a velocity slightly below 300 m/s (Fig. 11 and Fig. 14), corresponding to unconsolidated sand with few gravels as observed on site (Fig. 15). The velocity increases down to 60 m depth up to 500 m/s. A layer with this constant velocity is found down to 100 m depth. Below, the velocity increases up to 800 m/s at 200 m depth and 1000 m/s at 400 m depth. The interface with the bedrock is not well constrained between 400 and 550 m depth. Assuming the bedrock is dipping with a constant angle of 40° below the sediments, it would be found at 580 m depth in the centre of the array. Velocities in the bedrock of about 1800 m/s are retrieved but the confidence in this value is low.

When comparing to the target curves (Fig. 12 and Fig. 13), all dispersion curves are well represented.

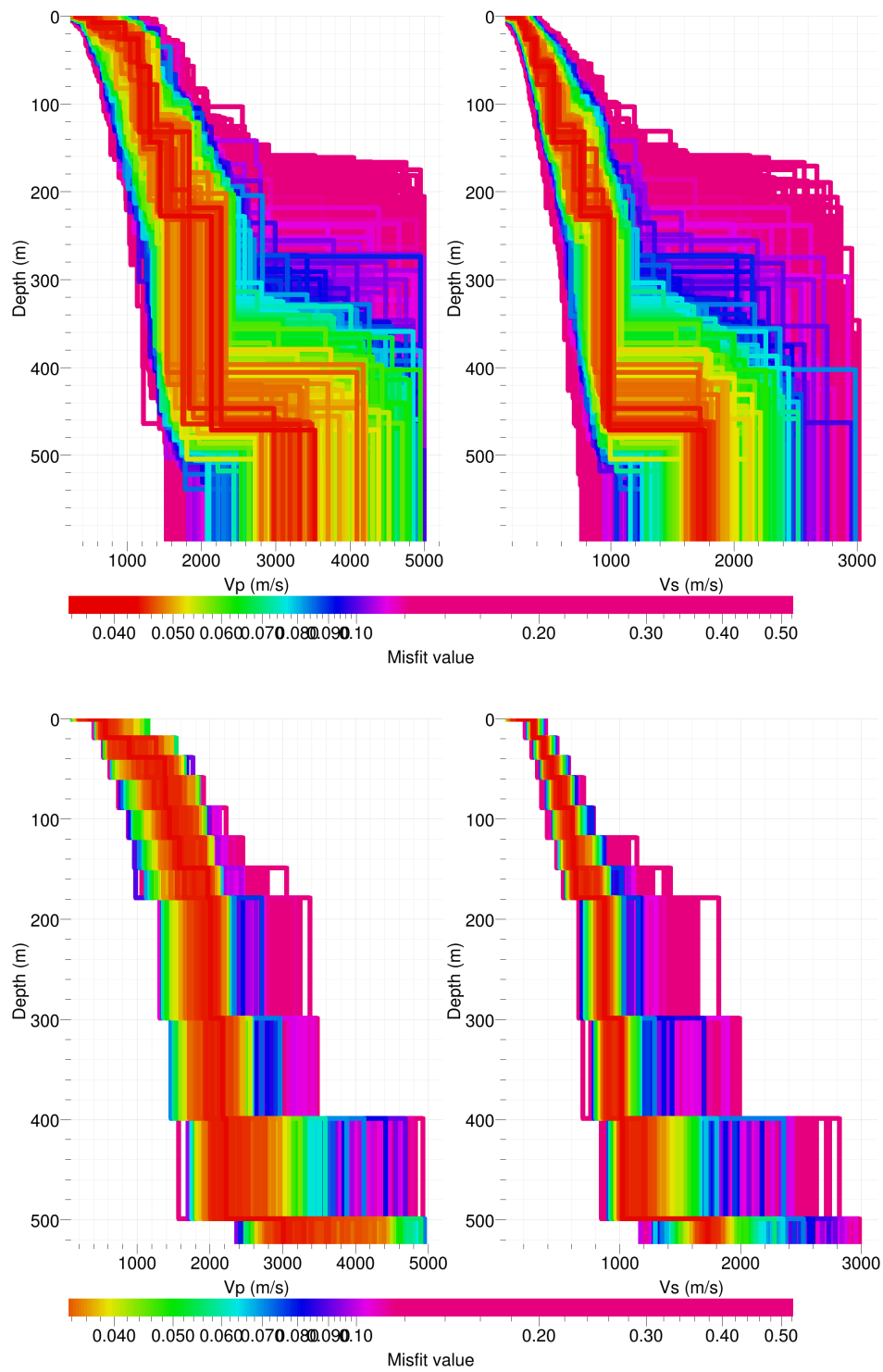


Figure 11: Inverted ground profiles in terms of  $V_p$  and  $V_s$ ; top: free layer depth strategy; bottom: fixed layer depth strategy.

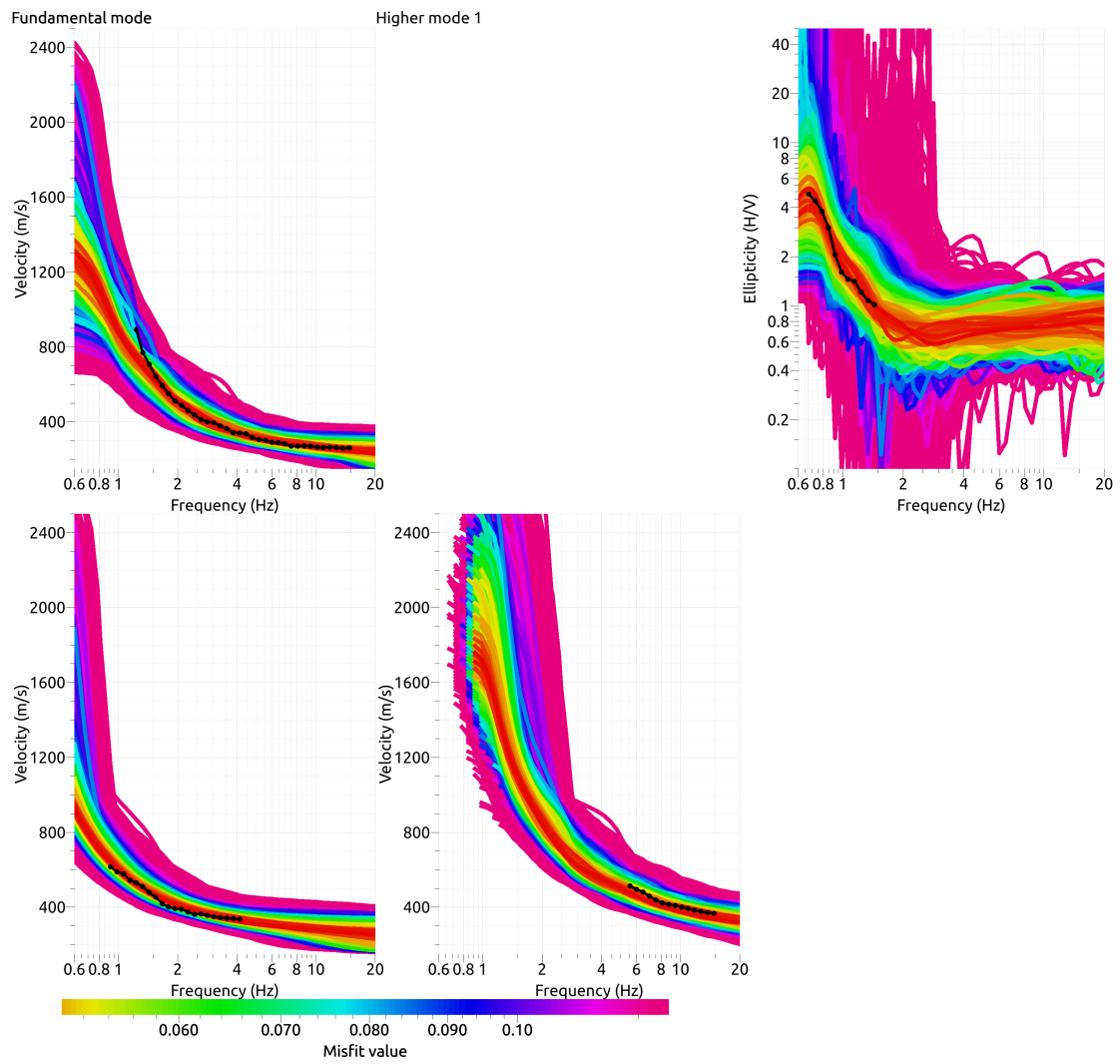


Figure 12: Comparison between inverted models and measured Rayleigh and Love modes and corresponding ellipticity, free layer depth strategy.

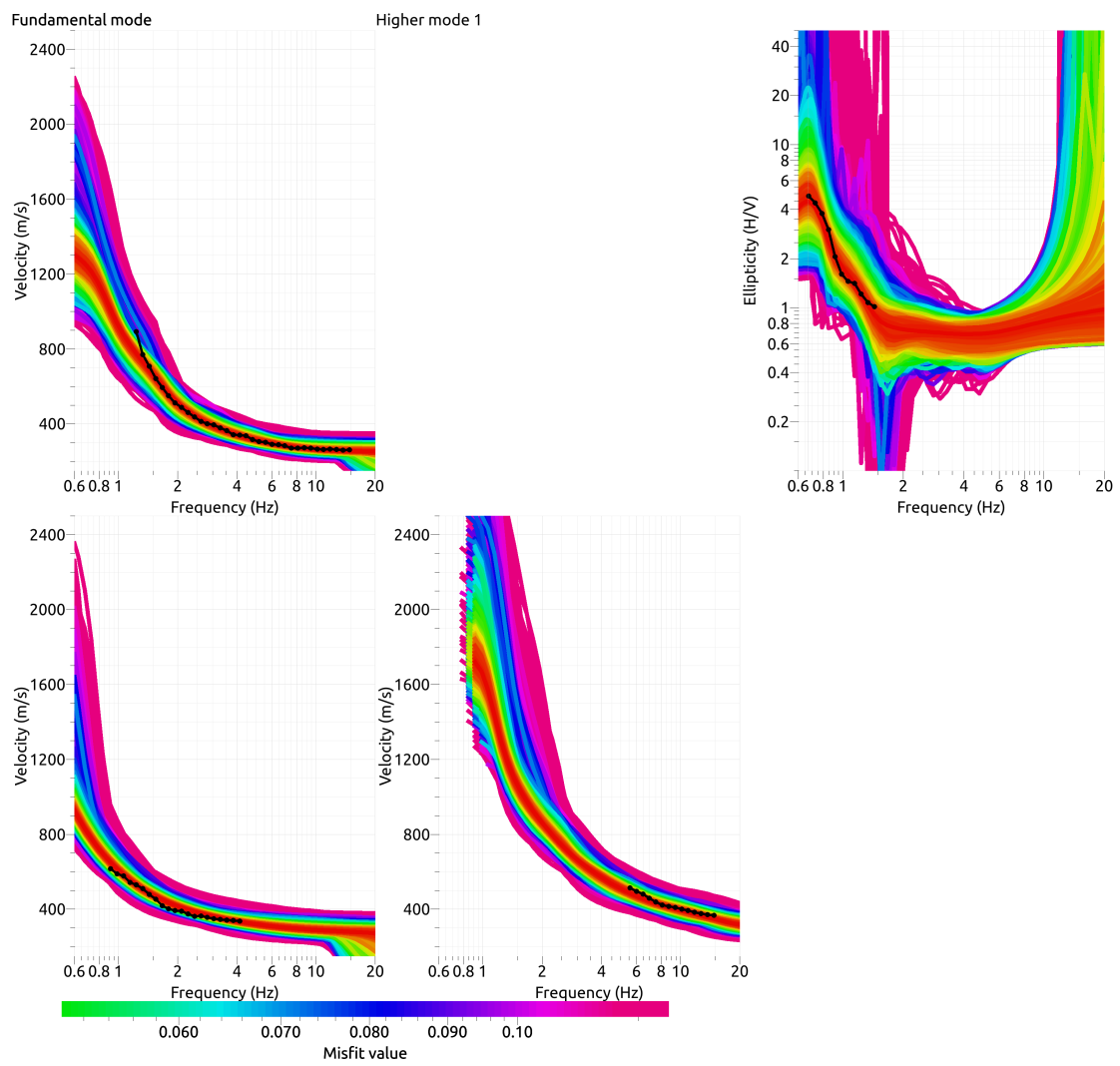


Figure 13: Comparison between inverted models and measured Rayleigh and Love modes and corresponding ellipticity, fixed layer depth strategy.

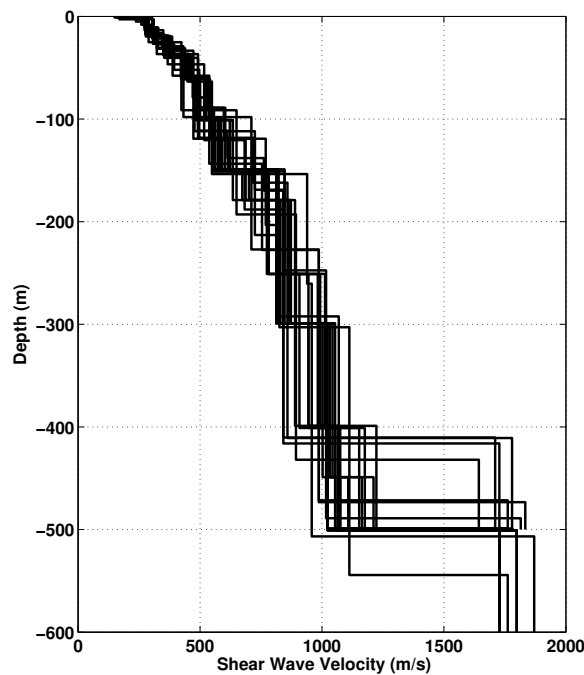


Figure 14:  $V_s$  ground profiles for the selected 25 best models.

## 6.2 Travel time average velocities and ground type

The distribution of the travel time average velocities at different depths was computed from the selected models. The uncertainty, computed as the standard deviation of the distribution of travel time average velocities for the considered models, is also provided, but its meaning is doubtful.  $V_{s,30}$  is found to be 304 m/s, which corresponds to class C in the Eurocode 8 [CEN, 2004] and SIA261 [SIA, 2003].

	Mean (m/s)	Uncertainty (m/s)
$V_{s,5}$	260	16
$V_{s,10}$	271	8
$V_{s,20}$	285	6
$V_{s,30}$	304	5
$V_{s,40}$	321	5
$V_{s,50}$	339	5
$V_{s,100}$	400	7
$V_{s,150}$	450	5
$V_{s,200}$	503	6

Table 7: Travel time averages at different depths from the inverted models. Uncertainty is given as one standard deviation from the selected profiles.



Figure 15: First meter of sediments from the works on the SLOP station.

### 6.3 SH transfer function and quarter-wavelength velocity

The quarter-wavelength velocity approach [Joyner et al., 1981] provides, for a given frequency, the average velocity at a depth corresponding to  $1/4$  of the wavelength of interest. It is useful to identify the frequency limits of the experimental data (minimum frequency in dispersion curves at 0.9 Hz and in the ellipticity curve at 0.7 Hz here). The results using this proxy show that the dispersion curves constrain the profiles down to 115 m and the ellipticity down to 170 m (Fig. 16). Moreover, the quarter wavelength impedance-contrast introduced by Poggi et al. [2012a] is also displayed in the figure. It corresponds to the ratio between two quarter-wavelength average velocities, respectively from the top and the bottom part of the velocity profile, at a given frequency [Poggi et al., 2012a]. It shows a trough (inverse shows a peak) at the resonance frequency.

Moreover, the theoretical SH-wave transfer function for vertical propagation [Roesset, 1970] is computed from the inverted profiles. It is compared to the quarter-wavelength amplification [Joyner et al., 1981] that however cannot take resonances into account (Fig. 17). In this case, the models are predicting a clear amplification up to a factor of 4 (with a reference rock at 1800 m/s), especially at resonance peaks at 1.1, 1.8 and 2.5 Hz. As a confirmation, a large peak in the ambient vibration spectra can be noticed also at 1.15 Hz.

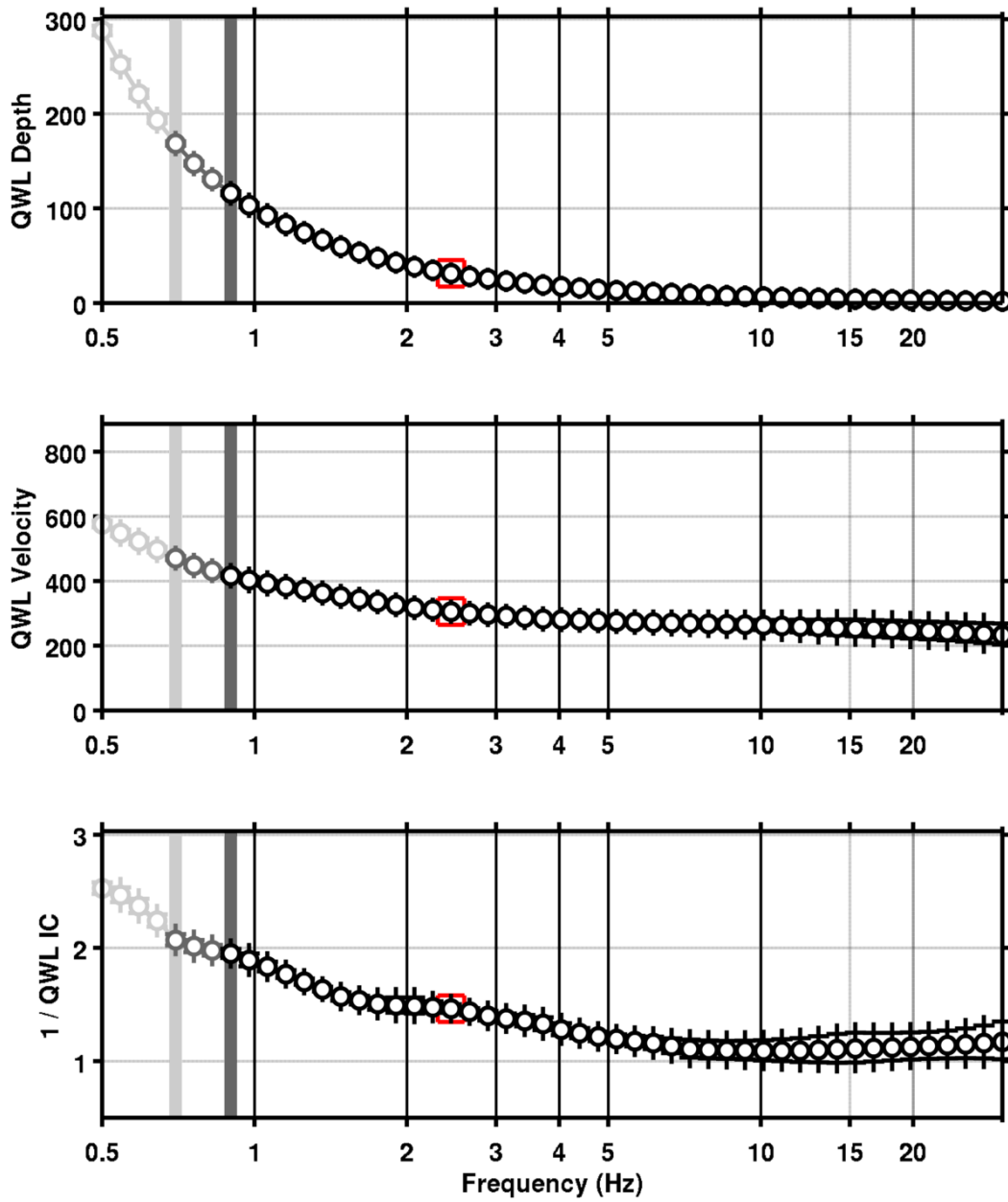


Figure 16: Quarter wavelength velocity representation of the velocity profile (top: depth, centre: velocity, bottom: inverse of the impedance contrast). Black curve is constrained by the dispersion curves, light grey is not constrained by the data. Red square is corresponding to  $V_{s,30}$ .

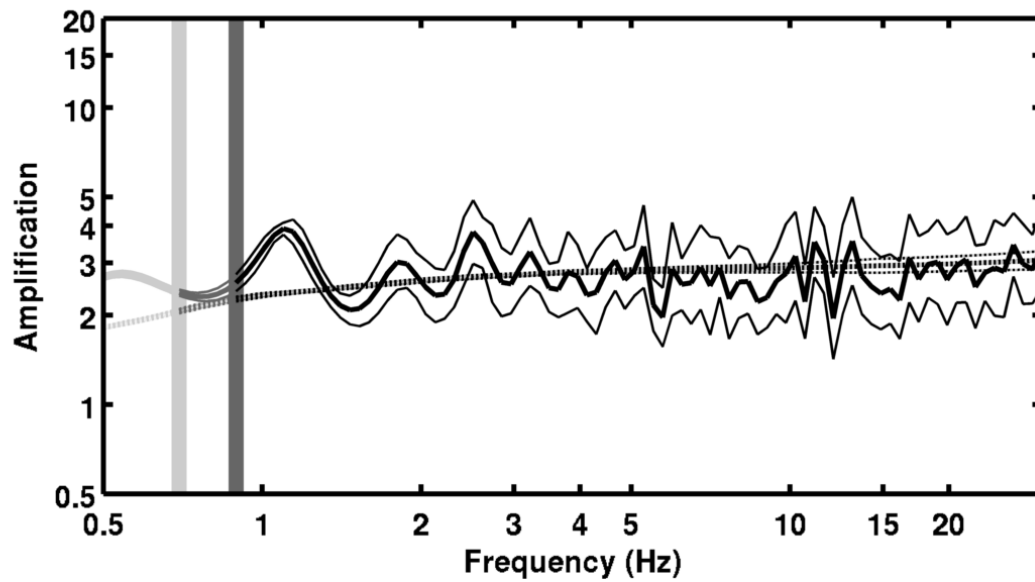


Figure 17: Theoretical SH transfer function (solid line) and quarter wavelength impedance contrast (dashed line) with their standard deviation. Significance of the greyshades is detailed in Fig. 16.

## 7 Conclusions

The array measurements presented in this study were successful in deriving a velocity model for the site of the SLOP station. The station is located on the alluvial fan of the Maggia river in the lake Maggiore basin. The sediment thickness in the city of Locarno is driving the fundamental H/V peak frequency down to 0.3 Hz, corresponding probably to more than 800 m of sediments. At the SLOP site, the H/V peak is at 0.67 Hz. The soil profile does not show clear interface. The first 10 – 20 m are made of unconsolidated sand with few gravels with a velocity slightly below 300 m/s. The velocity remains around 500 m/s down to 100 m depth. It reaches 800 m/s at 200 m depth and 1000 m/s at 400 m depth. The interface with the bedrock is not well constrained and between 400 and 550 m depth.

$V_{s,30}$  is 304 m/s, which would correspond to ground type C in the Eurocode 8 [CEN, 2004] and SIA261 [SIA, 2003]. The theoretical 1D SH transfer function and impedance contrast of the quarter-wavelength velocity computed from the inverted profiles show amplifications at clear resonance frequencies, especially at 1.1, 1.8 and 2.5 Hz. Recordings on the new station will allow to compare to these simple models.

## Acknowledgements

The authors thank Lea Kiefer who performed the single station measurements.

## References

- Sylvette Bonnefoy-Claudet, Fabrice Cotton, and Pierre-Yves Bard. The nature of noise wavefield and its applications for site effects studies. *Earth-Science Reviews*, 79(3-4): 205–227, December 2006. ISSN 00128252. doi: 10.1016/j.earscirev.2006.07.004. URL <http://linkinghub.elsevier.com/retrieve/pii/S0012825206001012>.
- Jan Burjánek, Gabriela Gassner-Stamm, Valerio Poggi, Jeffrey R. Moore, and Donat Fäh. Ambient vibration analysis of an unstable mountain slope. *Geophysical Journal International*, 180(2):820–828, February 2010. ISSN 0956540X. doi: 10.1111/j.1365-246X.2009.04451.x. URL <http://doi.wiley.com/10.1111/j.1365-246X.2009.04451.x>.
- J. Capon. High-Resolution Frequency-Wavenumber Spectrum Analysis. *Proceedings of the IEEE*, 57(8):1408–1418, 1969.
- CEN. *Eurocode 8: Design of structures for earthquake resistance - Part 1: General rules, seismic actions and rules for buildings*. European Committee for Standardization, en 1998-1: edition, 2004.
- Donat Fäh, Fortunat Kind, and Domenico Giardini. A theoretical investigation of average H / V ratios. *Geophysical Journal International*, 145:535–549, 2001.
- Donat Fäh, Gabriela Stamm, and Hans-Balder Havenith. Analysis of three-component ambient vibration array measurements. *Geophysical Journal International*, 172(1):199–213, January 2008. ISSN 0956540X. doi: 10.1111/j.1365-246X.2007.03625.x. URL <http://doi.wiley.com/10.1111/j.1365-246X.2007.03625.x>.
- Donat Fäh, Marc Wathelet, Miriam Kristekova, Hans-Balder Havenith, Brigitte Endrun, Gabriela Stamm, Valerio Poggi, Jan Burjanek, and Cécile Cornou. Using Ellipticity Information for Site Characterisation Using Ellipticity Information for Site Characterisation. Technical report, NERIES JRA4 Task B2, 2009.
- William B. Joyner, Richard E. Warrick, and Thomas E. Fumal. The effect of Quaternary alluvium on strong ground motion in the Coyote Lake, California, earthquake of 1979. *Bulletin of the Seismological Society of America*, 71(4):1333–1349, 1981.
- Katsuaki Konno and Tatsuo Ohmachi. Ground-Motion Characteristics Estimated from Spectral Ratio between Horizontal and Vertical Components of Microtremor. *Bulletin of the Seismological Society of America*, 88(1):228–241, 1998.
- Valerio Poggi and Donat Fäh. Estimating Rayleigh wave particle motion from three-component array analysis of ambient vibrations. *Geophysical Journal International*, 180(1):251–267, January 2010. ISSN 0956540X. doi: 10.1111/j.1365-246X.2009.04402.x. URL <http://doi.wiley.com/10.1111/j.1365-246X.2009.04402.x>.
- Valerio Poggi, Benjamin Edwards, and D. Fah. Characterizing the Vertical-to-Horizontal Ratio of Ground Motion at Soft-Sediment Sites. *Bulletin of the Seismological Society of America*, 102(6):2741–2756, December 2012a. ISSN 0037-1106. doi: 10.1785/0120120039. URL <http://www.bssaonline.org/cgi/doi/10.1785/0120120039>.

- Valerio Poggi, Donat Fäh, Jan Burjanek, and Domenico Giardini. The use of Rayleigh-wave ellipticity for site-specific hazard assessment and microzonation: application to the city of Lucerne, Switzerland. *Geophysical Journal International*, 188(3):1154–1172, March 2012b. ISSN 0956540X. doi: 10.1111/j.1365-246X.2011.05305.x. URL <http://doi.wiley.com/10.1111/j.1365-246X.2011.05305.x>.
- J.M. Roesset. Fundamentals of soil amplification. In R. J. Hansen, editor, *Seismic Design for Nuclear Power Plants*, pages 183–244. M.I.T. Press, Cambridge, Mass., 1970. ISBN 978-0-262-08041-5. URL <http://mitpress.mit.edu/catalog/item/default.asp?ttype=2&tid=5998>.
- SIA. *SIA 261 Actions sur les structures porteuses*. Société suisse des ingénieurs et des architectes, Zürich, sia 261:20 edition, 2003.
- Marc Wathelet. An improved neighborhood algorithm: Parameter conditions and dynamic scaling. *Geophysical Research Letters*, 35(9):1–5, May 2008. ISSN 0094-8276. doi: 10.1029/2008GL033256. URL <http://www.agu.org/pubs/crossref/2008/2008GL033256.shtml>.